

## Electromagnetic-Field Distribution Measurements in the Soft X-Ray Range: Full Characterization of a Soft X-Ray Laser Beam

S. Le Pape, Ph. Zeitoun, M. Idir, and P. Dhez

*Laboratoire de Spectroscopie Atomique et Ionique, Bâtiment 350, Université Paris-sud, 91405 Orsay, France*

J. J. Rocca

*Department of Electrical and Computer Engineering, Colorado State University, Fort Collins, Colorado 80523-1373*

M. François

*Institut d'Electronique et de Microélectronique du Nord, Université des Sciences et Technologie de Lille, avenue Poincaré BP 69, 59652 Villeneuve d'Ascq, France*

(Received 6 July 2001; published 18 April 2002)

We report direct measurement of the electromagnetic-field spatial distribution in a neonlike Ar capillary discharge-driven soft x-ray laser beam. The wave front was fully characterized in a single shot using a Shack-Hartmann diffractive optics sensor. The wave front was observed to be dependent on the discharge pressure and capillary length, as a result of beam refraction variations in the capillary plasma. The results predict  $\sim 70\%$  of the laser beam energy can be focused into an area 4 times the size of the diffraction-limited spot, reaching intensities of  $\sim 4 \times 10^{13}$  W/cm<sup>2</sup>.

DOI: 10.1103/PhysRevLett.88.183901

PACS numbers: 42.55.Vc, 41.50.+h, 52.58.Lq, 52.59.Ye

For several decades, synchrotrons have been used as soft x-ray sources for applications in disciplines ranging from biology [1] to solid state physics [2]. The past several years have witnessed the emergence of high brightness tabletop soft x-ray sources: high harmonic generation sources [3–5], and saturated soft x-ray lasers (SXRL) pumped by either fast capillary discharges [6] or optical lasers [7]. High order harmonics sources have been reported to generate radiation at wavelengths as short as 2.7 nm at 1 kHz repetition rate. Typically about  $10^8$  coherent photons per harmonic per pulse are generated in the spectral range from 50 to 13 nm in pulses as short as several femtoseconds. In turn, SXRL may produce very energetic pulses (more than  $10^{14}$  photons per pulse) at lower repetition rates. Saturated SXRL amplification has been achieved at wavelengths as short as 5.8 nm [8]. SXRL lasers have been used in several experiments that include the diagnostics of high density plasmas relevant to inertial confinement fusion [9], and spatial interferometry of a niobium surface deformed by an ultrahigh electric field [10]. Of particular interest for applications are tabletop capillary-discharge soft x-ray lasers that can be fired repetitively to generate an average power of several mW with a very high degree of spatial coherence [11].

The development of these tabletop coherent soft x-ray sources opens a wide field of applications in several disciplines using techniques such as interferometry, phase contrast imaging, and microscopy. Although an increase of the spatial coherence is important, the beam wave front must also be improved for such experiments. Indeed, imaging a sample with a phase contrast microscope and a coherent source having an aberrated wave front will result in a loss of resolution. On the other hand, wave front characterization can also impact applications such as two-photon

ionization in the soft x-ray range, which requires focusing of the beam into a spot of micrometer dimension to reach radiation intensities of the order of  $10^{13}$  W cm<sup>-2</sup>. Surprisingly, despite its key role in applications, the wave front of tabletop soft x-ray sources had not been measured prior to this work. A technique frequently used to obtain aberration-free wave fronts consists in spatially filtering the beam by placing a small pinhole (typically  $\sim 1$   $\mu$ m diam [12]) at the focal spot of a focusing optic. However, since in most cases the incoming beam is aberrated, the filtered beam power is reduced by several orders of magnitude compared to the incoming beam [12]. In contrast, coherent beam brightness might be greatly increased by directly optimizing the source parameters to improve the beam wave front. Such development requires detailed maps of the wave fronts.

With this objective, we have developed an extreme ultraviolet (EUV) Shack-Hartmann wave front sensor. The sensor is an extrapolation to the soft x-ray range of a technique used in the visible spectral range [13]. In related work, a point source diffraction interferometer has been previously realized to test EUV lithography optics using synchrotron radiation [14]. The Shack-Hartmann wave front sensor is based on mapping the wave vectors at numerous locations across the wave front. The beam pupil is sampled by a matrix of lenslets, each focusing a small fractional area of the laser beam onto a detector. The focal spot positions are directly related to the local wave front slope, whereas the spot intensity is associated with the local electric field amplitude. Such a diagnostic allows the reconstruction of the electromagnetic field in a single shot measurement. The measurements reported herein allowed the full characterization of the electromagnetic field distribution in a tabletop capillary discharge pumped soft x-ray

laser operating at a wavelength of 46.9 nm ( $\lambda_{\text{SXRL}}$ ) in the  $3s^1P_1-3p^1S_0$  line of Ne-like Ar [6]. The gain medium is an elongated plasma column generated in a capillary channel by a fast discharge current pulse. The magnetic force of the current pulse rapidly compresses the plasma to form a dense and hot column with length-to-diameter ratios of nearly 1000:1. Gain saturation is reached after amplification in a  $\sim 14$ – $15$  cm long column. The capillary length used in most of the present experiment was 35 cm, which corresponds to a highly saturated amplifier. The output energy increases by nearly a factor of 10 while the plasma column is elongated from 16 to 35 cm.

Figure 1 illustrates the experimental setup used in the wave front measurements. The wave front sensor was placed at 2.5 m from the capillary end in order to optimize the spatial sampling of the beam. The soft x-ray Shack-Hartmann wave front sensor is composed of an array of 200 diffractive lenses working in reflection at an incidence angle of  $22.5^\circ$ . Diffractive lenses were chosen because they do not generate aberration while working off axis. The lenses that have a radius of  $700 \mu\text{m}$  were etched on a 1 in. diam flat silicate substrate. Each lens has nine circular grooves, the outer one with a width of  $26 \mu\text{m}$ . The groove's height was selected such that the waves reflected from the bottom and from the top of the groove profile are in phase, leading to the highest focusing efficiency. A  $1000 \text{ \AA}$  layer of iridium was coated on the entire substrate surface to provide  $\sim 10\%$  reflectivity. The selected focal length of 50 cm leads to a resolution on the wave front slope of  $0.1 \mu\text{rad}$ , corresponding to  $\lambda_{\text{SXRL}}/300$  on the wave front. The focal spots were recorded with a cooled back-illuminated CCD array of  $1300 \times 1340$  pixels placed at the focal plane of the lenses. The capillary discharge SXRL is sufficiently powerful to record high contrast images in a single shot, avoiding errors that otherwise might possibly arise from shot-to-shot variations. In fact, the laser beam had to be significantly attenuated to avoid saturation of the detector. This was accomplished without altering the wave front by leaking a controlled amount of Ar gas in the detector chamber. Figure 1 includes an image acquired in the focal plane of the lens array, displaying the array of focal spots corresponding to each of the microlenses. To obtain absolute wave front measurements, it is crucial to measure wave front distortions that can be caused by the substrate using a spherical wave front. Indeed, the lenses are etched on a 6-mm thick substrate, where deformations can induce an artificial shift of the focal spots. The substrate planarity is  $\lambda/20$  with  $\lambda = 0.6 \mu\text{m}$ , which is equivalent to  $0.7\lambda_{\text{XRL}}$ . In addition, the stress caused by the mirror holder can cause deformations of several  $\lambda_{\text{XRL}}$  of amplitude. We created a reference spherical wave front by diffracting the laser beam with a  $10 \mu\text{m}$  diameter pinhole placed at 2.2 m from the sensor. The absolute SXRL wave front is obtained by subtraction of this reference wave from the laser wave front. A comparison of the positions of

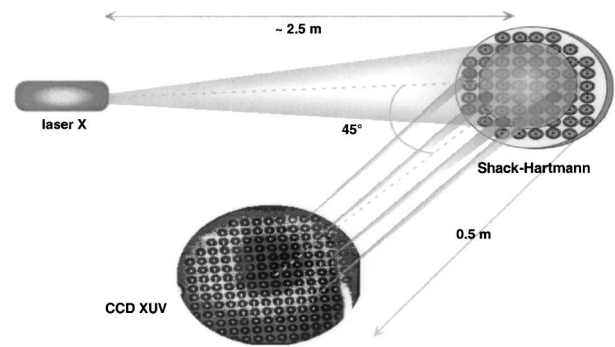


FIG. 1. Schematic representation of the experimental setup showing an image of the lens array and corresponding image of focal spots. The angle between the incident and reflected beams is  $45^\circ$ . The lighter parts of the image correspond to the brighter part of the beam.

the focal spots corresponding to the reference wave with a regular mesh clearly showed an increasing displacement of the focal spots from the beam center to the side, resulting from the increasing wave front slope on the side of the spherical wave.

Since the x-ray laser under study is fully coherent, there is a unique phase relation between every point on the detector, and, consequently, the wave front shape can be reconstructed from the focal spot positions shown in Fig. 1. A program was developed to estimate each focal spot centroid with an accuracy of about  $10^{-2}$  pixels. The wave front was subsequently reconstructed with a second program based on the algorithm written by Southwell [13]. The phase in each point was calculated by using a Gauss-Seidel method, which has been chosen for its convergence speed and its accuracy. The accuracy of the wave front reconstruction is  $10^{-3}\lambda_{\text{XRL}}$ .

We have investigated the variation of the wave front characteristics as a function of the argon pressure in the capillary discharge laser channel. The results of measurements corresponding to discharge pressures of 200, 420 (near the optimum for maximum laser power), and 660 mTorr are shown in Fig. 2. The Shack-Hartmann wave front sensor allows the detection of aberration amplitudes of  $1/100$  of the maximum peak. For all pressures, the wave front is nearly a divergent spherical wave with a curvature radius of almost 6.5 m. The wave front shape and radius are observed to be dominantly determined by beam refraction in the discharge-pumped amplifier induced by the radial electron density gradient in the capillary plasma column [15]. It is also refraction that dominantly determines the annular beam shape observed in Fig. 2a. Two general trends are observed for each pressure: (i) The wave front is smoother in the center of the beam; (ii) the amplitude of wave front defects decreases as the pressure is increased (from  $7\lambda_{\text{XRL}}$  rms at 200 mTorr, to  $3\lambda_{\text{XRL}}$  rms at 660 mTorr). The defects are evaluated by subtracting the XRL wave front from a best-fit spherical wave front. This decrease in wave front aberration at increased pressure results from the smoother electron density gradients

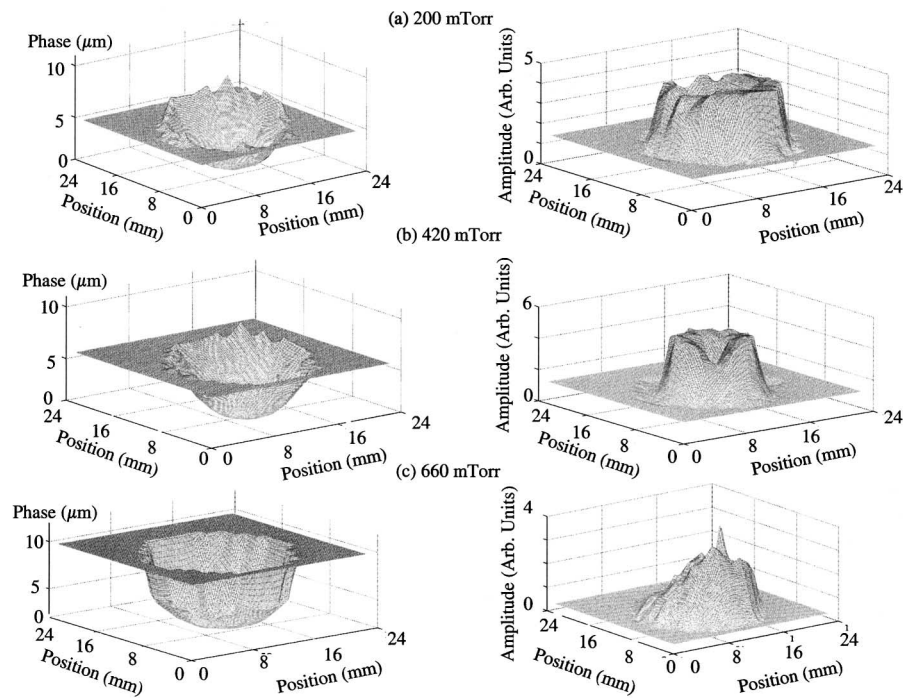


FIG. 2. Wave front shape (left) and corresponding intensity distributions (right) for different discharge pressures [(a)–(c)]. The radius of curvature of the wave front is 6.5 m. The annular shape of the beam at the lower pressures is due to increased refraction.

and reduced refraction that are a consequence of reduced plasma column compression at the higher discharge pressures. The XRL shot-to-shot wave front stability was also investigated making several measurements for each pressure. The shot-to-shot wave front variation was determined to be  $0.22\lambda_{\text{XRL}}$ .

The measured wave front characteristics discussed above, which correspond to a 35 cm long capillary, were used to simulate the intensity distribution of the laser beam at the focal spot of an  $f = 50$  mm diffraction-limited optic. Notice that if we had used only the measurement of the wave front shape the energy distribution in the focal plane would have been inexact, as it results from the convolution of the wave front shape with the intensity distribution in the beam. The energy distribution in the focal plane was calculated for the three different pressures at which the wave front and the corresponding intensity distribution were measured. The results are shown in Figs. 3a–3c. The most notable changes are observed in the intensity distribution at the foot of the beam, and are a result of the wave front improvement at the higher pressures [from  $7\lambda_{\text{XRL}}$  rms at 200 mTorr in Fig. 3a to  $3\lambda_{\text{XRL}}$  rms at 660 mTorr in Fig. 3c]. At the pressure of 660 mTorr, the focal spot diameter is estimated to be approximately  $0.3 \mu\text{m}$ , and increases in size as the pressure is reduced reaching  $0.7 \mu\text{m}$  at a pressure of 200 mTorr. Of particular interest are the results of Fig. 3b, corresponding to the nearly optimum laser operating pressure of 420 mTorr at which laser pulse energies approaching 1 mJ can be generated. At this pressure the distribution exhibits a strong peak that includes 70% of the total laser beam energy in a

$0.5 \mu\text{m}$  focal spot. The focal spot is estimated to be only 5 times larger than the area of a diffraction-limited beam, corresponding to an intensity of about  $4 \times 10^{13} \text{ W cm}^{-2}$  assuming one reflecting surface with 50% reflectivity. In contrast, significantly shorter capillary lengths were observed to result in a much larger focal spot. Figure 4 shows the energy distribution in the focal plane for an 18 cm long capillary discharge operated at 420 mTorr. In this case, the energy is spread out over a surface area of about  $70 \times 70 \mu\text{m}^2$ , with large secondary peaks caused by strong aberrations on the SXRL wave front. About 5% of the total energy in the beam is focused onto a  $4 \mu\text{m}$  diameter focal spot. This result is in good agreement with a previous focusing experiment [16], where  $\sim 3\%$  of the beam energy was focused onto a  $2 \mu\text{m}$  diameter focal spot. At the time of the experiment, it was not possible to perform the same measurement but for the longest capillary due to the need to sample the focal spot with an accuracy of typically  $0.03 \mu\text{m}$ . The improvement of the focusing characteristics of the beams generated by the longer capillaries is a result of the spatial filtering induced by beam refraction in the capillary. This effect is also responsible for the previously observed enhancement of the degree of spatial coherence with capillary length.

In summary, we have measured for the first time the absolute electromagnetic field of a soft x-ray laser. A soft x-ray Shack-Hartmann sensor was used to gather in a single shot the data required for the reconstruction of the electromagnetic field corresponding to a capillary discharge soft x-ray laser. The results suggest it should be possible to focus the output of capillary discharge lasers

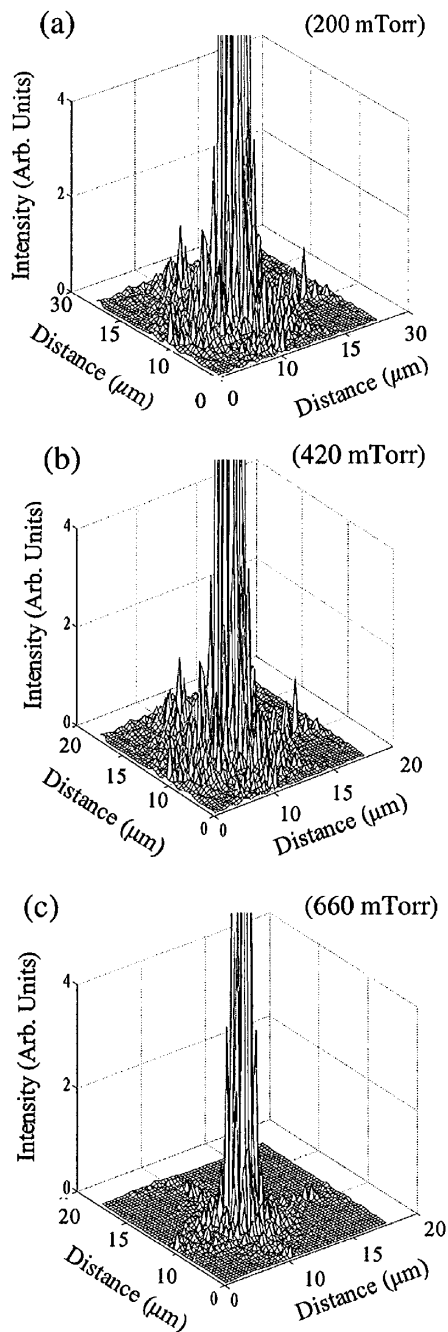


FIG. 3. Simulated beam intensity distributions of the laser beam of a 35 cm long capillary discharge at the focal spot of an  $f = 50$  mm diffraction-limited optics for three different discharge pressures. The figure shows zooms of the foot of the focal spot. The ratio between peak and foot amplitude ( $1/20$ ) is selected to be the same in all cases.

onto near diffraction-limited spots, achieving unprecedented soft x-ray power densities. The use of this technique to obtain detailed knowledge of the electromagnetic field distribution of different tabletop short wavelength sources will allow their improvement for use in a new variety of applications ranging from phase contrast imaging a beam focusing onto submicron focal spots.

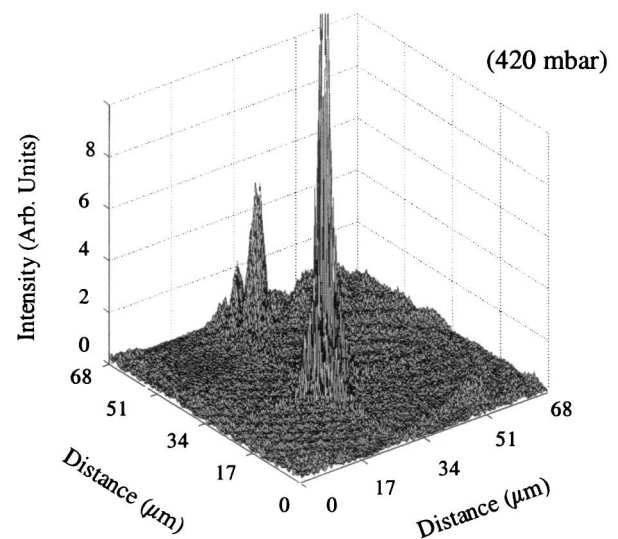


FIG. 4. Simulated beam intensity distribution of the laser beam produced by an 18 cm long capillary discharge at the focal spot of an  $f = 50$  mm diffraction-limited optics for a discharge pressure of 420 mTorr.

This work was supported by the National Science Foundation, the U.S. Department of Energy, Chemical Sciences, Geosciences and Biosciences Division of the Office of Basic Energy Sciences, and by the contract NSF/CNRS No. 9153. We also acknowledge support from the W.M. Keck Foundation.

- 
- [1] C. A. Larabell, D. Yager, and M. Meyer-Ilse, in *Proceedings of the Sixth International Conference on X-ray Microscopy, Berkeley, 1999*, edited by W. Meyer-Ilse, T. Warwick, and D. Attwood (American Institute of Physics, New York, 2000), p. 107.
  - [2] S. Hüfner, *Photoelectron Spectroscopy* (Springer-Verlag, Berlin, 1996), 2nd ed.
  - [3] A. L'Huillier and Ph. Balcou, *Phys. Rev. Lett.* **59**, 56 (1987).
  - [4] Z. Chang *et al.*, *Phys. Rev. Lett.* **79**, 2967 (1997).
  - [5] A. Rundquist *et al.*, *Science* **280**, 1412 (1998).
  - [6] B. R. Benware *et al.*, *Phys. Rev. Lett.* **81**, 5804 (1998).
  - [7] J. Dunn *et al.*, *Phys. Rev. Lett.* **84**, 4834 (2000).
  - [8] R. Smith *et al.*, *Phys. Rev. A* **59**, R47 (1999).
  - [9] L. B. Da Silva *et al.*, *Phys. Rev. Lett.* **74**, 3991 (1995).
  - [10] Ph. Zeitoun *et al.*, *Nucl. Instrum. Methods Phys. Res., Sect. A* **416**, 189 (1998).
  - [11] Y. Liu *et al.*, *Phys. Rev. A* **63**, 033802 (2001).
  - [12] D. Attwood, in *Soft X-rays and Extreme Ultraviolet Radiation: Principles and Applications* (Cambridge University, Cambridge, England, 2000), p. 318.
  - [13] W. H. Southwell, *J. Opt. Soc. Am.* **70**, 8 (1980).
  - [14] H. Medeck, E. Tejnil, K. Goldberg, and J. Bokor, *Opt. Lett.* **21**, 1526 (1996).
  - [15] C. H. Moreno *et al.*, *Phys. Rev. A* **58**, 1509 (1998).
  - [16] B. R. Benware *et al.*, *Opt. Lett.* **24**, 1714 (1999).